Do Liposomal Apoptotic Enhancers Increase Tumor Coagulation and End-Point Survival in Percutaneous Radiofrequency Ablation of Tumors in a Rat Tumor Model?[1]

Wei Yang, MD, PhD
Muneeb Ahmed, MD
Mostafa Elian, MD
El-Shymma A. Hady, MD
Tatyana S. Levchenko, PhD
Rupa R. Sawant, PhD
Sabina Signoretti, MD
Michael Collins, BS
Vladimir P. Torchilin, PhD
S. Nahum Goldberg, MD

Purpose: To characterize effects of combining radiofrequency (RF) ablation with proapoptotic intravenous liposome-encapsulated paclitaxel and doxorubicin on tumor destruction, apoptosis and heat-shock protein (HSP) production, intratumoral drug accumulation, and end-point survival.

Materials and Methods: R3230 mammary adenocarcinomas (n = 177) were implanted in 174 rats in this animal care committee–approved study. Tumors received *(a)* no treatment, *(b)* RF ablation, *(c)* paclitaxel, *(d)* RF ablation followed by paclitaxel (RF ablation–paclitaxel), *(e)* paclitaxel before RF ablation (paclitaxel–RF ablation), *(f)* RF ablation followed by doxorubicin (RF ablation–doxorubicin), *(g)* paclitaxel followed by doxorubicin without RF ablation (paclitaxel-doxorubicin), or *(h)* paclitaxel before RF ablation, followed by doxorubicin (paclitaxel–RF ablation–doxorubicin). Tumor coagulation area and diameter were compared at 24–96 hours after treatment. Intratumoral paclitaxel uptake with and without RF ablation were compared. Immunohistochemical staining revealed cleaved caspase-3 and 70-kDa HSP (HSP70) expression. Tumors were randomized into eight treatment arms for Kaplan-Meier analysis of defined survival end-point (3.0-cm diameter).

Results: Paclitaxel–RF ablation increased tumor coagulation over RF ablation or paclitaxel (mean, 14.0 mm ± 0.9 [standard deviation], 6.7 mm ± 0.6, 2.5 mm ± 0.6, respectively; $P < .001$). Paclitaxel–RF ablation–doxorubicin had similar tumor coagulation ($P < .05$), compared with paclitaxel–RF ablation, at 24 and 96 hours. Mean intratumoral paclitaxel accumulation for paclitaxel–RF ablation (6.76 μg/g ± 0.35) and RF ablation–paclitaxel (9.28 μg/g ± 0.87) increased over that for paclitaxel (0.63 μg/g ± 0.25, $P < .001$). Paclitaxel substantially increased apoptosis and decreased HSP70 expression at coagulation margin. Mean end-point survival for paclitaxel–RF ablation–doxorubicin (56.8 days ± 25.3) was greater, compared with that for paclitaxel–RF ablation or RF ablation–paclitaxel (17.6 days ± 2.5), RF ablation–doxorubicin (30.3 days ± 4.9, $P < .002$), or paclitaxel-doxorubicin (27.9 days ± 4.1, $P < .001$).

Conclusion: Selecting adjuvant liposomal chemotherapies (paclitaxel, doxorubicin) to target cellular apoptosis and HSP production effectively increases RF ablation–induced tumor coagulation and end-point survival, and combined multidrug approach results in even better outcomes.

Supplemental material: *http://radiology.rsna.org/lookup/suppl/doi:10.1148/radiol.10100500/-/DC1*

[1] From the Laboratory for Minimally Invasive Tumor Therapies, Department of Radiology, Beth Israel Deaconess Medical Center/Harvard Medical School, 330 Brookline Ave, Boston, MA 02215 (W.Y., M.A., M.E., E.S.A.H., S.N.G.); Division of Image-guided Therapy, Department of Radiology, Hadassah Hebrew University Medical Center, Jerusalem, Israel (S.N.G.); Key Laboratory of Carcinogenesis and Translational Research (Ministry of Education), Department of Ultrasound, Peking University School of Oncology, Beijing Cancer Hospital and Institute, Beijing, China (W.Y.); Department of Pharmaceutical Sciences and Center for Pharmaceutical Biotechnology and Nanomedicine, Northeastern University, Boston, Mass (T.L., R.R.S., V.P.T.); Department of Pathology, Brigham and Women's Hospital, Boston, Mass (S.S., M.C.); and Department of Radiology, El Minia University, El Minia, Egypt (M.E., S.A.H.). Received March 7, 2010; revision requested April 14; final revision received June 16; final version accepted June 18. W.Y. supported by Chinese National High Technology Research and Development Program 863, Commission No. 2007AA02Z4B8. **Address correspondence to** M.A. (e-mail: *mahmed@bidmc.harvard.edu*).

Radiofrequency (RF) ablation of solid tumors has been progressively adopted widely into clinical practice for small (<3.0-cm-diameter) tumors because of its high effectiveness and low risk of complications (1–4). However, a key limitation of this technique remains the incomplete treatment of larger tumors, which often leads to local tumor recurrence (5–7). Specifically, researchers in several studies (8–11) have reported residual tumor growth, suggesting the persistence of microscopic foci of viable tumor at the margin of the target ablation zone. One potential strategy to overcome the current limitations of performing RF ablation alone is the addition of adjuvant treatments, such as chemotherapy or radiation therapy (12–14). Indeed, investigators in several studies (15–18) have demonstrated complementary interactions when they combined RF ablation and concurrent administration of the chemotherapeutic agent doxorubicin, particularly in the form of a liposomal preparation. Researchers in mechanistic studies (19–21) have further shown that liposomal doxorubicin increases effectiveness of ablation, in part by cellular stress leading to apoptosis, but also produces heat-shock proteins (HSPs), such as 70-kDa HSP (HSP70), which have been shown to limit tissue damage. Therefore, other compounds that have greater apoptosis potential and/or HSP suppression hold the potential to further increase RF ablation–induced tissue coagulation.

Along these lines, paclitaxel is one possible agent for use in combination with RF ablation, as it is an increasingly used chemotherapeutic agent with low toxicity in clinical practice that has confirmed strong apoptotic effects, as well as inhibition of HSP formation, and can be incorporated into a liposomal preparation (22–26). Thus, we hypothesized that increased tumor coagulation and hence end-point survival after treatment with a combination of RF ablation and liposomal paclitaxel might be better than other treatment strategies, including RF ablation with liposomal doxorubicin. Despite this mechanistic rationale, to our knowledge, intratumoral uptake for liposomal paclitaxel combined with RF ablation and the potential effects on apoptosis, tumor destruction, and survival are unknown. Furthermore, researchers in prior studies have demonstrated the influence of key parameters, such as the timing between the administration of adjuvant liposomal doxorubicin therapy and RF ablation, both in terms of the amount of intratumoral drug uptake and tumor coagulation (27). Hence, further characterization of the parameters for the new treatment adjuvant (liposomal paclitaxel) is also required.

Accordingly, the purpose of our study was fourfold: *(a)* to characterize and compare tumor necrosis induced by various treatment regimens combining RF ablation with or without liposomal paclitaxel and/or doxorubicin, *(b)* to determine whether RF ablation increases intratumoral accumulation of liposomal paclitaxel; *(c)* to explore

Advances in Knowledge

- Radiofrequency (RF) ablation combined with nanoparticle-delivered adjuvant chemotherapeutic agents, such as liposomal paclitaxel, can be successfully used to target specific cellular pathways, such as apoptosis enhancement and heat-shock protein (HSP) suppression, to increase tumor destruction and animal end-point survival.
- Administration of adjuvant intravenous (IV) liposomal paclitaxel in combination with RF ablation increases the amount of apoptosis observed in periablational zone tissue that has been previously shown to recover from reversible cellular injury from exposure to sublethal hyperthermia.
- RF ablation combined with two adjuvant IV liposomal drugs (paclitaxel and doxorubicin) further improves animal end-point survival compared with the use of either agent alone, suggesting a synergistic inhibitory effect of combination liposomal paclitaxel and doxorubicin on tumor growth.
- Greater suppression of 70-kDa HSP expression is seen with liposomal paclitaxel compared with doxorubicin, suggesting that an additional benefit of paclitaxel to combination therapy may also be an effect of HSP suppression.

Implication for Patient Care

- The results of our study underscore the potential role and ultimate clinical benefit of combining RF ablation with tailored adjuvant nanoparticle-encapsulated chemotherapies that target and modulate specific cellular mechanisms.
- Characterizing potential adjuvant agents that target separate pathways alone and in combination may ultimately allow for an interventional oncology strategy that includes administering multiple drugs with synergistic effects to maximize tumoricidal effect and improve overall clinical treatment effectiveness.

Published online before print
10.1148/radiol.10100500

Radiology 2010; 257:685–696

Abbreviations:
HSP = heat-shock protein
HSP70 = 70-kDa HSP
IHC = immunohistochemistry
IV = intravenous
RF = radiofrequency

Author contributions:
Guarantors of integrity of entire study, M.A., S.N.G.; study concepts/study design or data acquisition or data analysis/interpretation, all authors; manuscript drafting or manuscript revision for important intellectual content, all authors; approval of final version of submitted manuscript, all authors; literature research, W.Y., M.A., M.E., V.P.T., S.N.G.; clinical studies, M.E.; experimental studies, W.Y., M.E., T.S.L., R.R.S., S.S., M.C., V.P.T., S.N.G.; statistical analysis, W.Y., M.A., M.E., S.N.G.; and manuscript editing, W.Y., M.A., M.E., V.P.T., S.N.G.

Funding:
This research was supported by the National Cancer Institute, National Institutes of Health (grants R01CA133114, R01 CA100045, and 2R01 HL55519).

Authors stated no financial relationship to disclose.

the potential effects of these regimens on RF ablation–induced apoptosis and HSP formation with immunohistochemical (IHC) staining, and *(d)* to investigate the benefit of combination treatment on end-point survival in a small-animal tumor model.

Materials and Methods

Experimental Overview

Approval of the Institutional Animal Care and Use Committee (Beth Israel Deaconess Medical Center, Boston, Mass) was obtained before the start of our study. This study was performed in four phases to systematically investigate the potential synergistic effects of RF ablation with adjuvant liposomal paclitaxel and/or doxorubicin. A total of 177 tumors in 174 animals were used.

Phase 1: Characterization of tumor destruction in combination therapy with liposomal paclitaxel and/or doxorubicin.—A total of 98 tumors in 98 animals were used in this phase. For our first experiment, the time course of coagulation from two different liposomal paclitaxel administration strategies was determined. Fifty-two tumors randomly received standardized RF ablation (1-cm tip, 5 min, 70°C) and intravenous (IV) liposomal paclitaxel (volume, 0.5 mL; dose, 0.06 mg) 24 hours before RF ablation (hereafter referred to as paclitaxel–RF ablation) or 15 minutes after RF ablation (hereafter referred to as RF ablation–paclitaxel). The animals in these two groups were sacrificed at 0, 4, 24, 72, and 96 hours after the last treatment (n = 5–6 in each subgroup).

Next, we compared tumor coagulation 4 and 24 hours after the last treatment for eight experimental groups: *(a)* no treatment; *(b)* RF ablation alone; *(c)* administration of IV liposomal paclitaxel alone; *(d)* RF ablation–paclitaxel; *(e)* paclitaxel–RF ablation; *(f)* RF ablation, followed 15 minutes later by administration of IV liposomal doxorubicin (volume, 0.5 mL; dose, 1 mg) (hereafter referred to as RF ablation–doxorubicin); *(g)* administration of IV liposomal paclitaxel, followed by administration of IV liposomal doxorubicin without RF ablation (hereafter referred to as paclitaxel-doxorubicin); and *(h)* IV liposomal paclitaxel administered 24 hours before RF ablation, followed 15 minutes later by administration of IV liposomal doxorubicin (hereafter referred to as paclitaxel–RF ablation–doxorubicin). The coagulation data for the RF ablation alone and RF ablation–doxorubicin groups were obtained from tumors stored in a tumor bank of the same tumor model treated under similar conditions (28), whereas the coagulation data for the RF ablation–paclitaxel and paclitaxel–RF ablation groups came from the time course study above. Therefore, an additional 36 tumors were used (groups: no treatment, paclitaxel alone, paclitaxel-doxorubicin, paclitaxel–RF ablation–doxorubicin; n = 3 for sacrifice at 4 hours, n = 6 for sacrifice at 24 hours). An additional 10 tumors were treated with paclitaxel–RF ablation and paclitaxel–RF ablation–doxorubicin to permit comparison of tumor coagulation at 96 hours after the last treatment. For all groups, gross histopathologic analysis and comparison of tumor coagulation were performed.

Phase 2: Quantification of intratumoral paclitaxel accumulation.—We performed quantitative analysis of the amount of intratumoral paclitaxel achieved from administration of liposomal paclitaxel with and without RF ablation. A total of 15 tumors in 12 rats were used for this phase. Four groups were used (n = 12 tumors, nine animals): *(a)* control (no treatment), *(b)* paclitaxel alone, *(c)* paclitaxel–RF ablation, and *(d)* RF ablation–paclitaxel. For three animals with two paired tumors each, one tumor of each pair was treated with RF ablation–paclitaxel, whereas the other tumor was used as an internal control that was not treated with RF ablation. The tumor to be treated with RF ablation was randomly selected to minimize potential selection bias. Three animals with single tumors were treated with paclitaxel–RF ablation. These six animals were sacrificed at 24 hours following RF ablation (for paclitaxel–RF ablation–treated tumors, this is 48 hours after drug injection). This time was selected because findings in prior studies demonstrated that maximum intrahepatic liposomal doxorubicin uptake occurred 24 hours after RF ablation (27). The remaining three animals with single tumors did not receive any treatment and served as negative controls. On the basis of initial results, to enable determination of intratumoral paclitaxel when paclitaxel was given alone (ie, without RF ablation), it was necessary to give an additional three animals a double dose (1.0 mL) and double concentration (0.24 mg/mL) in a repeat experiment, with linear estimation (ie, dividing by four) to approximate the standard-dose intratumoral drug uptake.

Phase 3: IHC characterization of distribution and expression of apoptosis and HSP production.—On the basis of the results above, we used 32 representative tumor samples from the experiments above harvested at 4 or 24 hours after the last treatment from three treatment groups and one control group for IHC staining (n = 3–5, each subgroup). These groups included: *(a)* paclitaxel alone, *(b)* paclitaxel–RF ablation, *(c)* paclitaxel–RF ablation–doxorubicin, and *(d)* no treatment. In addition, 16 recut samples from RF ablation alone and RF ablation–doxorubicin groups (n = 3–5, each subgroup) from a previously generated tissue bank in this model were used as supplemental control groups. As an additional control to ensure uniformity of staining, whenever direct comparisons were made, IHC staining was repeated with all relevant comparative slides stained at the same time. Tissues were stained with hematoxylin-eosin for gross histopathologic analysis and with cleaved caspase-3 (Cell Signaling Technology, Danvers, Mass) for apoptosis and HSP70 (Stressgen HSP70 ELISA kit; Assay Designs, Ann Arbor, Mich) for heat-shock analysis, as previously described (28).

Phase 4: Tumor growth rates and end-point survival.—To investigate end-point survival and tumor growth from different treatment strategies, 64 tumors or rats (one tumor per rat) were randomized into the same eight experimental groups used in phase 1 (n = 8 each, described in detail above): *(a)* no treatment, *(b)* RF ablation alone, *(c)* paclitaxel

alone, *(d)* RF ablation–paclitaxel, *(e)* paclitaxel–RF ablation, *(f)* RF ablation–doxorubicin, *(g)* paclitaxel-doxorubicin, or *(h)* paclitaxel–RF ablation–doxorubicin. The survival end point was a tumor diameter of 30 mm or survival of 90 days, whichever was reached first. Secondary end points were rate of tumor growth and local control (ie, no visible tumor on the chest wall).

Animal Model

For all experiments and procedures, anesthesia was induced with intraperitoneal injection of a mixture of ketamine (Ketaject; Phoenix Pharmaceutical, St Joseph, Mo) at a dose of 50 mg/kg and xylazine (Bayer, Shawnee Mission, Kan) at 5 mg/kg. Animals were sacrificed with an overdose of pentobarbital sodium (Nembutal; Abbott Laboratories, Chicago, Ill) at a dose of 0.2 mL/kg.

Experiments were performed with a well-characterized established R3230 mammary adenocarcinoma cell line used in multiple prior studies (29–31). In total, 174 Fischer rats with R3230 tumors were used in this study. Fresh tumor was initially harvested from a live carrier. Within 30 minutes of this tumor explantation, the tumor was homogenized with a tissue grinder (model 23; Kontes Glass, Vineland, NJ) with an aseptic technique and suspended in 7 mL of Roswell Park Memorial Institute (RPMI) 1640 medium (Biomedicals, Aurora, Ill). One or two tumors (as specified above) were implanted into each animal with direct visualization by using 0.3–0.4 mL of tumor suspension injected slowly via an 18-gauge needle into the mammary fat pad of female Fischer rats (mean weight, 120 g ± 20 [standard deviation]; age range, 13–14 weeks) obtained from a supplier (Taconic Farms, Germantown, NY); the strain of animals used in the experiments was the same as that from which this tumor was derived initially. Animals were maintained on an ad lib diet (standard rodent chow 8664; Harlan-Teklab, Baltic, Conn) and were monitored every 2–3 days to measure tumor growth. Only solid, nonnecrotic tumors (as determined at ultrasonography at the time of treatment) that were 1.2–1.6 cm in the largest diameter were used for this study. Tumors were grown for 14–21 days until the desired size was achieved, at which point they were randomized to one of the treatment arms. In addition, after enrollment in survival studies, tumor diameters were measured every day in the longitudinal and transverse directions with mechanical calipers (W.Y., M.E.). Accuracy of the final measurement was verified by the senior author (S.N.G.), who was blinded to treatment group.

RF Application

Conventional monopolar RF ablation was applied by using a 500-kHz RF ablation generator (model 3E; Radionics, Burlington, Mass). To complete the RF circuit, the animal was placed on a standardized metallic grounding pad (Radionics). Contact was ensured by shaving the animal's back and by liberally applying electrolytic contact gel. Initially, the 1-cm tip of a 21-gauge electrically insulated electrode (SMK electrode; Radionics) was placed at the center of the tumor. RF current was applied for 5 minutes with the generator output titrated to maintain a designated mean tip temperature (70°C ± 2), with a mean current of 90.2 mA ± 22.8 and a range of 49–157 mA. This standardized method of RF ablation application has been demonstrated previously to provide reproducible coagulation volumes with use of this conventional RF ablation system (17,30).

Liposomal Agent Preparation

We used a commercially available preparation of liposomal doxorubicin (Doxil; Alza Pharmaceuticals, Palo Alto, Calif). For this study, we purposefully used the taxol derivative formulation that could be maximally concentrated into liposomal vehicles similar to previously used liposomal doxorubicin. The paclitaxel liposomes were prepared such that the lipid composition in these liposomes was identical to that of liposomal doxorubicin, as has been described in previous work (30). Briefly, 0.12 mg of paclitaxel (10 mg/mL solution in methanol) was added to a mixture of egg phosphatidylcholine, cholesterol, and PEG2000-PE (57.25:37.57:5.18 mol %, respectively) solutions in chloroform, and a lipid film was formed in a round-bottom flask by using solvent removal on a rotary evaporator. The lipid film was then rehydrated with 1 mL of phosphate-buffered saline, pH 7.4, and the preparation was probe-sonicated (Sonic Dismembrator model 100; Fisher Scientific, Pittsburgh, Pa) at a power output of 7 W for 30 minutes. To remove any titanium particles that may have been shed from the tip of the probe during sonication, the sample was centrifuged for 10 minutes at 2000 rpm (32). The agent was injected within 24 hours of formulation, during which time it was maintained at room temperature. The drug concentration was not measured at the time of injection.

Intravenous Administration of Liposomal Agents

Liposomal paclitaxel was injected slowly (0.5-mL IV dose per animal for 30 seconds via a 27-gauge needle) into the tail vein at the selected administration time (either 24 hours before RF ablation or 15 minutes after RF ablation) at the maximum liposomal saturation dose (0.12 mg paclitaxel). Liposomal doxorubicin was injected with the same approach 15 minutes after RF ablation in the combined-therapy group. The doxorubicin dose was 1 mg (0.5-mL IV dose of a 2 mg/mL concentration preparation).

Measurement of Intratumoral Paclitaxel

At sacrifice and excision, tumors were embedded immediately in optimum cutting temperature compound (Fisher Scientific, Pittsburgh, Pa), frozen in liquid nitrogen, and stored at −80°C prior to paclitaxel uptake analysis. Tumor samples were homogenized (Yamato Laboratory Stirrer; Yamato Scientific America, Santa Clara, Calif) in 0.5 mL of deionized water. The drug was then extracted into 1 mL of *tert*-butyl methylether by vortexing for 30 minutes. After centrifugation at 13500 rpm for 5 minutes, the clear supernatant (0.8 mL) was removed and evaporated under a gentle stream of nitrogen. The residue was then dissolved by 0.2 mL of mobile phase, centrifuged at 13500 rpm for 1 minute,

and injected onto a high-performance liquid chromatography column. A high-performance liquid chromatography system equipped with a diode array and fluorescence detector (D-7000; Hitachi, Tokyo, Japan) and column that was 4.6 × 250 mm (Spherisorb ODS2; Waters, Milford, Mass) were used. The column was eluted with an acetonitrile-water reagent (65:35 vol/vol) at 1.0 mL/min. Paclitaxel was detected at 227 nm. The injection volume was 50 μL (33).

Gross Histopathologic Analysis

As previously reported, staining was performed to assess tumor destruction via assessment of mitochondrial enzyme activity by incubating thin tissue sections in 2% 2,3,5-triphenyltetrazolium chloride (Fisher Scientific, Fairlawn, NJ) for 30 minutes (29,34). With this assessment method, viable tissue with intact mitochondrial enzyme activity is stained red, while ablated tissue does not have a red color (35). The extent of visible coagulation was measured in two separate and perpendicular dimensions with calipers. The coagulation diameter (ie, longest measurement perpendicular to the inserted electrode) in all tissue samples was determined in a blinded fashion by three authors (W.Y., M.E., S.N.G., with 2, 2, and 12 years of experience, respectively). For histopathologic analysis, tumors were sectioned perpendicularly to the direction of electrode insertion and placed in cassettes containing the central section of tumor. All tissue was fixed in 10% formalin overnight at 4°C, embedded in paraffin, and sectioned at a thickness of 5 μm.

IHC Staining

The 5-μm sections were placed on positively charged microscope slides (Superfrost Plus; Fisher Scientific, Pittsburgh, Pa) and incubated overnight at 37°C and for 1 hour at 58°C. At paraffin removal and tissue rehydration, slides were heated with a microwave oven at 97°C for 10 minutes for retrieval of antigenic activity. Sections were incubated with hydrogen peroxide at room temperature for 5 minutes to inactivate endogenous peroxidase. IHC assays were performed by using antibodies on each sample to detect cleaved caspase-3, a marker of apoptosis (36), and HSP70, a key product of the HSP chain (37). Sections were incubated with primary antibodies at room temperature for 60 minutes and washed with phosphate-buffered saline. Sections were then incubated with species-matched secondary antibodies at room temperature for 30 minutes. Nuclear counterstaining was performed lightly with hematoxylin-eosin. Sections were dehydrated, and cover slips were applied by using mounting medium (Permount; Richard-Allan Scientific, Kalamazoo, Mich).

Stained slides were imaged and analyzed by using a microscope (Micromaster I; Westover Scientific, Mill Creek, Wash) with imaging software (Micron; Westover Scientific). Temporal evolution of cellular morphologic characteristics and the spatial distribution of protein expression were determined in relation to the central zone of RF coagulation and to one another. Quantitative analysis was performed by using two metrics: the average thickness of the rim of staining and the percentage of cells that stain per high-power (×40) field within the defined zone (28). Five random high-power fields were analyzed for a minimum of three specimens for each parameter and were assigned scores in a blinded fashion to remove observer bias. Accuracy of the final data was verified by the senior author (S.N.G.), who was blinded to treatment group.

Statistical Analysis

Software (SPSS 13.0; SPSS, Chicago, Ill) was used for statistical analysis in the current study. All data were provided as the mean ± standard deviation. Paclitaxel uptake, tumor destruction, and IHC staining results were compared by using analysis of variance and the Student *t* test. The Kaplan-Meier method and log-rank test were used for end-point survival analysis. Mean and median times were used for end-point survival analysis. Differences with *P* values of less than .05 were considered significant.

Results

Phase 1: Characterization of Tumor Destruction in Combination RF Ablation Therapy with Liposomal Paclitaxel and/or Doxorubicin

Paclitaxel–RF ablation increased tumor coagulation over RF ablation or paclitaxel alone at 24 hours (mean, 14.0 mm ± 0.9, 6.7 mm ± 0.6, and 2.5 mm ± 0.6,

Figure 1

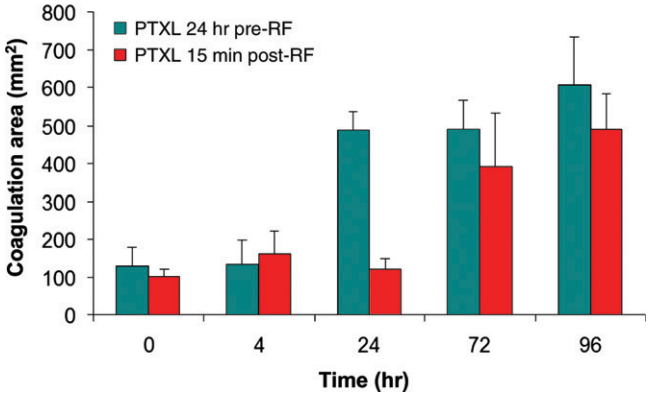

Figure 1: Comparison of effect of paclitaxel *(PTXL)* timing (either before RF ablation *[pre-RF]* or after RF ablation *[post-RF]*) on tumor coagulation over time. Tumor coagulation increased over time for both groups (paclitaxel–RF ablation and RF ablation–paclitaxel) to a similar maximum amount at 96 hours ($P = .16$). More rapid response was observed for paclitaxel–RF ablation, which had the greatest rate of mean increase in coagulation area occurring earlier (4–24 hours, 352.5 mm² ± 81.2) compared with that at later time (24–72 hours, 258.9 mm² ± 158.9) for RF ablation–paclitaxel.

respectively; $P < .001$ for all comparisons). Similarly, paclitaxel–RF ablation resulted in a greater area of tumor coagulation (mean, 488.4 mm^2 ± 48.7) compared with that for RF ablation alone (mean, 138.8 mm^2 ± 12.7; $P < .001$). Both RF ablation–paclitaxel and paclitaxel–RF ablation resulted in equivalent coagulation area at 96 hours (mean, 589.4 mm^2 ± 108.7 and 490.5 mm ± 92.6, respectively; $P = .16$). However, significant differences were seen between the rapidity of response between the two dosing regimens, with a greater rate of increase in coagulation area occurring earlier for paclitaxel–RF ablation (from 4 hours to 24 hours: mean, 352.5 mm^2 ± 81.2), compared with a later time frame for RF ablation–paclitaxel (from 24 hours to 72 hours: mean, 258.9 mm^2 ± 158.9) (Fig 1). Paclitaxel–RF ablation–doxorubicin resulted in a maximum coagulation diameter similar to that for paclitaxel–RF ablation (mean, 14.3 mm ± 1.1 and 14.0 mm ± 0.9, respectively; $P = .563$) but resulted in greater overall area of coagulation at 24 hours after treatment (mean, 595.9 mm^2 ± 80.9 and 488.4 mm^2 ± 48.7, respectively; $P = .016$) (Fig E1 [online]). However, at 96 hours after treatment, no difference was seen between paclitaxel–RF ablation–doxorubicin and paclitaxel–RF ablation for either coagulation diameter (mean, 14.5 mm ± 1.0 and 15.2 mm ± 0.8, respectively; $P = .24$) or area (mean, 587.5 mm^2 ± 83.8 and 575.6 mm^2 ± 93.5, respectively; $P = .83$).

Phase 2: Quantification of Intratumoral Paclitaxel Accumulation

We observed a substantial increase in intratumoral drug uptake in tumors treated with RF ablation combined with paclitaxel compared with tumors that received the drug alone (Table 1). RF ablation sharply increased the intratumoral paclitaxel accumulation in RF ablation–paclitaxel (mean, 9.28 μg/g ± 0.87) and paclitaxel–RF ablation (mean, 6.76 μg/g ± 0.35), compared with the estimated intratumoral paclitaxel concentration of paclitaxel alone (mean, 0.63 μg/g ± 0.25; $P < .001$). Between these two combination groups, RF ablation–paclitaxel had higher intratumoral drug accumulation compared with that for paclitaxel–RF ablation ($P = .01$). Of note, initial measurements of intratumoral paclitaxel for tumors treated with paclitaxel alone were below our 0.1 μg/mL detection level. Therefore, as noted in Methods, an additional three animals were administered a double dose and double concentration. This increased drug dose resulted in a mean of 2.53 μg/g ± 1.01, corresponding to an estimated 0.63 μg/g ± 0.25.

Phase 3: IHC Characterization of Distribution and Expression of Apoptosis and HSP Production

Although minimal scattered cellular apoptosis was seen at 24 hours in tumors treated with liposomal paclitaxel alone, there was no increase in staining for apoptosis or HSPs in a defined spatial distribution pattern. However, for the RF ablation combination groups, IHC staining revealed bands of discrete cleaved caspase-3 situated adjacent to the zone of coagulation and a ring of HSP70 immediately peripheral to the rim of cleaved caspase-3 staining.

Compared with RF ablation alone, both paclitaxel–RF ablation and RF ablation–doxorubicin independently substantially increased apoptosis at the margin of coagulation, but peak apoptotic expression occurred at different times (4 hours for RF ablation–doxorubicin

Table 1

Increase in Intratumoral Accumulation of Liposomal Paclitaxel with RF Ablation

Group	Dose (mL)	Time after Paclitaxel (h)	Paclitaxel Uptake (μg/g)*
Control	0.5	...	0
Paclitaxel alone	0.5	24	Undetectable
PaclitaxeL alone†	0.5†	24	0.63 ± 0.25
Paclitaxel–RF ablation	0.5	48	6.76 ± 0.35
RF ablation–paclitaxel	0.5	24	9.28 ± 0.87

Note.—RF ablation increased intratumoral liposomal paclitaxel accumulation for any dosing regimen (24 hours before and 15 minutes after RF ablation) over paclitaxel alone ($P < .001$, all comparisons). Intratumoral liposomal paclitaxel accumulation was significantly greater for liposomal paclitaxel administered 15 minutes after RF ablation compared with liposomal paclitaxel administered 24 hours before RF ($P = .01$).

* Data are the means ± standard deviations unless otherwise specified.

† The intratumoral drug concentration for a regular dose of IV liposomal paclitaxel administered alone was initially undetectable and was subsequently estimated after higher dosing, as detailed in Materials and Methods where phase 2 is discussed.

Table 2

Quantitative IHC Staining for Apoptosis

	4 Hours		24 Hours	
Group	Rim Thickness (mm)	Positive Cells (%)	Rim Thickness (mm)	Positive Cells (%)
Paclitaxel	...	...	...	...
RF ablation	0.49 ± 0.12	48.9 ± 7.0	No rim	No rim
RF ablation–doxorubicin	0.70 ± 0.13*	71.6 ± 2.8*	0.18 ± 0.08	45.2 ± 9.2
Paclitaxel–RF ablation	0.54 ± 0.16	56.1 ± 5.6	0.90 ± 0.57*	81.3 ± 7.8*
Paclitaxel–RF ablation–doxorubicin	0.58 ± 0.05	60.2 ± 6.8	0.26 ± 0.11	50.7 ± 4.2

Note.—Data are the means ± standard deviations unless otherwise specified. RF ablation–doxorubicin and paclitaxel–RF ablation significantly increased cleaved caspase-3 staining over RF ablation alone, with peak apoptotic expression at different times (4 hours for RF ablation–doxorubicin and 24 hours for paclitaxel–RF ablation [$P < .001$, both comparisons]). Cleaved caspase-3 rim thickness was greatest (0.9 mm), but had the most variability (± 0.57 mm) for paclitaxel–RF ablation at 24 hours. Cleaved caspase-3 was higher with paclitaxel–RF ablation–doxorubicin than with RF ablation alone at both times, but lower than RF ablation–doxorubicin at 4 hours ($P < .005$) and paclitaxel–RF ablation at 24 hours ($P < .001$).

* Significantly greater values compared with values for all other treatments listed ($P < .05$).

and 24 hours for paclitaxel–RF ablation) (Table 2). The cleaved caspase-3 rim thickness was greatest (0.9 mm) but had the most variability (± 0.57 mm) for paclitaxel–RF ablation at 24 hours where intense positive staining was seen, even extending to the margin in one tumor with a 1.98-mm thickness (Fig 2). The mean value for cleaved caspase-3 was higher in the paclitaxel–RF ablation–doxorubicin group than in the group with RF ablation alone at both times but lower than that for the RF ablation–doxorubicin group at 4 hours (rim thickness, 0.58 mm ± 0.05 and 0.70 mm ± 0.13, respectively; percentage of positive cells, 60.2% ± 6.8 and 71.6% ± 2.8, respectively; $P < .005$), and the mean value for the paclitaxel–RF ablation–doxorubicin group was lower than that for the paclitaxel–RF ablation group at 24 hours (rim thickness, 0.26 mm ± 0.11 and 0.90 mm ± 0.57, respectively; percentage of positive cells, 50.7% ± 4.2 and 81.3% ± 7.8, respectively; $P < .001$).

In regard to HSP70 expression, adjuvant paclitaxel resulted in a reduction in HSP70 staining (no obvious or minimal staining) at 4 hours compared with that for RF ablation alone; in comparison, increased HSP70 staining was observed with RF ablation–doxorubicin (mean rim thickness, 0.68 mm ± 0.07 vs 0.43 mm ± 0.04; mean percentage of positive cells, 60.2% ± 5.4 vs 35.6% ± 4.3; $P < .001$), but this was substantially diminished at 4 hours with the addition of paclitaxel (paclitaxel–RF ablation–doxorubicin) (Table 3, Fig 3). There was no obvious rim or minimal staining for both paclitaxel–RF ablation and paclitaxel–RF ablation–doxorubicin groups at 4 hours, suggesting increased suppression at early times. By 24 hours, persistent HSP70 was detected in RF ablation alone and RF ablation–doxorubicin groups (mean rim thickness, 0.71 mm ± 0.18 and 0.64 mm ± 0.17, respectively; mean percentage of positive cells, 78.3% ± 3.9 and 67.4% ± 4.3, respectively). A variable but comparatively diminished rim of staining of HSP70 did develop in three of five paclitaxel–RF ablation tumors and in all paclitaxel–RF ablation–doxorubicin tumors at 24 hours (mean rim thickness, 0.37 mm ± 0.24

Figure 2

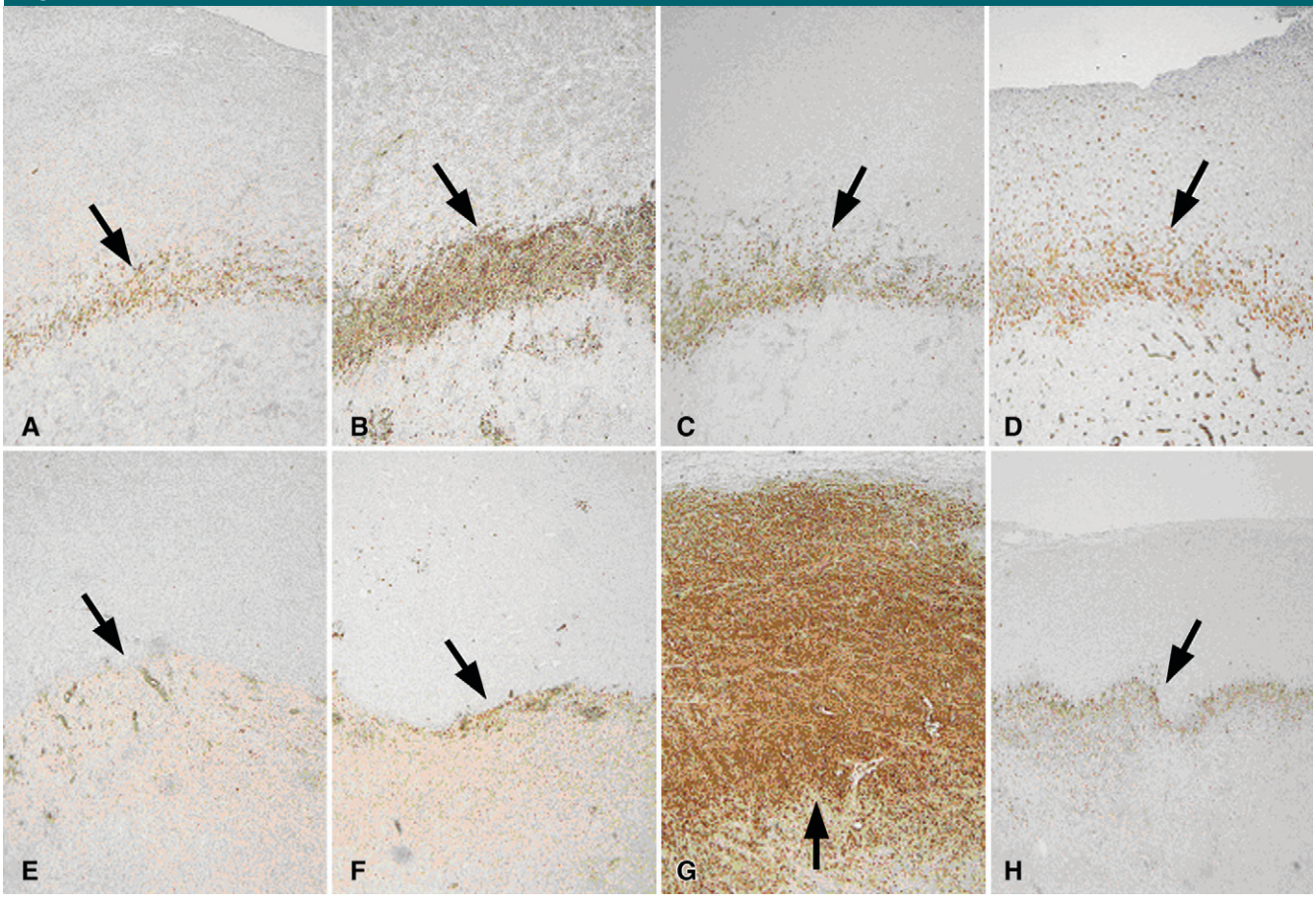

Figure 2: Apoptosis following combined RF ablation and liposomal chemotherapy. *A–H,* Photomicrographs show rim staining of cleaved caspase-3 (arrows) surrounding zone of coagulation. (Original magnification, ×4.) *A–D,* Sections from tumors excised at 4 hours. *E–H,* Sections from tumors excised at 24 hours. *A, E,* RF ablation alone. *B, F,* RF ablation–doxorubicin. *C, G,* Paclitaxel–RF ablation. *D, H,* Paclitaxel–RF ablation–doxorubicin. At 4 hours, RF ablation–doxorubicin demonstrated the strongest staining for cleaved caspase-3 expression. At 24 hours, paclitaxel–RF ablation demonstrated the greatest overall staining, seen extending to tumor margin on *G.*

and 0.52 mm ± 0.22, respectively; mean percentage of positive cells, 43.2% ± 32.2 and 53.7% ± 24.2, respectively; $P < .005$). The other two of five tumors in the paclitaxel–RF ablation group had virtually no HSP70 staining at 24 hours.

Phase 4: Tumor Growth Rates and End-Point Survival

Mean and median survival for rats that received RF ablation and single-agent therapy (paclitaxel–RF ablation, RF ablation–paclitaxel, or RF ablation–doxorubicin) were greater (mean and median, 18.9 days ± 3.4 and 18 days, 17.6 days ± 2.5 and 17.5 days, and 30.3 days ± 4.9 and 30 days, respectively) than they were for rats that received RF ablation alone (mean and median, 14.9 days ± 1.8 and 15 days, respectively), paclitaxel alone (mean and median, 13.1 days ± 2.5 and 12 days, respectively), or for rats in the control group (mean and median, 10.4 days ± 1.5 and 10 days, respectively; $P < .02$, all comparisons). However, animals that received combined RF ablation–doxorubicin survived longer than did animals that received combined RF ablation and paclitaxel ($P < .005$). There was no significant difference in mean end-point survival between earlier (24 hours before) and later (15 minutes after) paclitaxel administration. Overall, triple therapy (paclitaxel–RF ablation–doxorubicin) showed the greatest end-point survival (mean and median, 56.8 days ± 25.3 and 45.5 days, respectively) (Fig 4), with corresponding slower tumor growth rates (Fig 5). The latter value was significantly greater than it was for RF ablation combined with either paclitaxel (mean, 17.6 days ± 2.5 and 18.9 days ± 3.4, respectively; $P < .001$, all comparisons) or doxorubicin (30.3 ± 4.9 days, $P < .002$). In addition, local control occurred in two tumors treated with paclitaxel–RF ablation–doxorubicin but not in tumors in any other treatment groups (Fig E2 [online]).

Table 3

Quantitative IHC Staining for HSP Expression

	4 Hours		24 Hours	
Group	Rim Thickness (mm)	Positive Cells (%)	Rim Thickness (mm)	Positive Cells (%)
Paclitaxel	...	...	...	...
RF ablation	0.43 ± 0.04	35.6 ± 4.3	0.71 ± 0.18	78.3 ± 3.9
RF ablation–doxorubicin	0.68 ± 0.07*	60.2 ± 5.4*	0.64 ± 0.17	67.4 ± 4.3
Paclitaxel–RF ablation	...†	...†	0.37 ± 0.24‡	43.2 ± 32.2‡
Paclitaxel–RF ablation–doxorubicin	...†	...†	0.52 ± 0.22‡	53.7 ± 24.2‡

Note.—Data are the means ± standard deviations unless otherwise specified. Increased HSP70 staining was observed with RF ablation–doxorubicin compared with RF alone ($P < .001$), and was substantially diminished at 4 hours with the addition of paclitaxel (paclitaxel–RF ablation–doxorubicin) ($P < .005$).

* Significant increase of RF ablation–doxorubicin compared with RF ablation alone.

† There was no rim or minimal HSP70 expression for both paclitaxel–RF ablation groups and paclitaxel–RF ablation–doxorubicin at 4 hours, suggesting increased suppression at early times.

‡ By 24 hours, persistent HSP70 was detected in RF ablation alone and RF ablation–doxorubicin groups, with reduced staining for paclitaxel–RF ablation and paclitaxel–RF ablation–doxorubicin ($P < .005$).

Discussion

Several investigators have reported the use of pharmacologic agents as adjuvants to RF ablation in an attempt to increase treatment volumes and improve clinical outcomes. In particular,

Figure 3

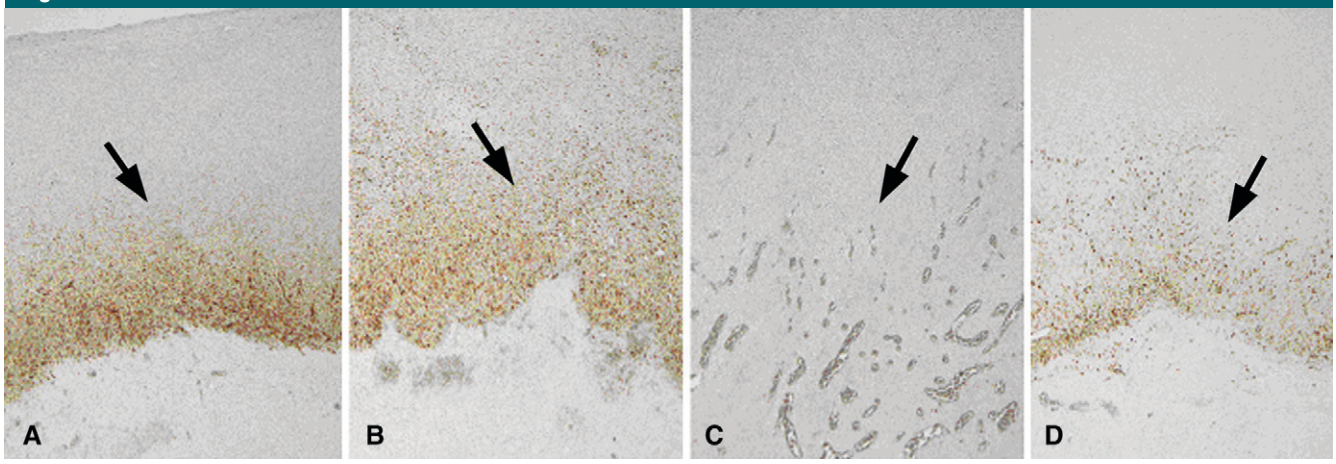

Figure 3: HSP production following combined RF ablation and liposomal chemotherapy. *A–D,* Photomicrographs show rim staining of HSP70 (arrows) surrounding zone of coagulation on sections from tumors excised at 24 hours. (Original magnification, ×4.) *A,* RF ablation alone. *B,* RF ablation–doxorubicin. *C,* Paclitaxel–RF ablation. *D,* Paclitaxel–RF ablation–doxorubicin. HSP70 staining was substantially diminished in tumors treated with paclitaxel–RF ablation, with a comparatively less intensely positive rim observed for paclitaxel–RF ablation–doxorubicin.

Figure 4

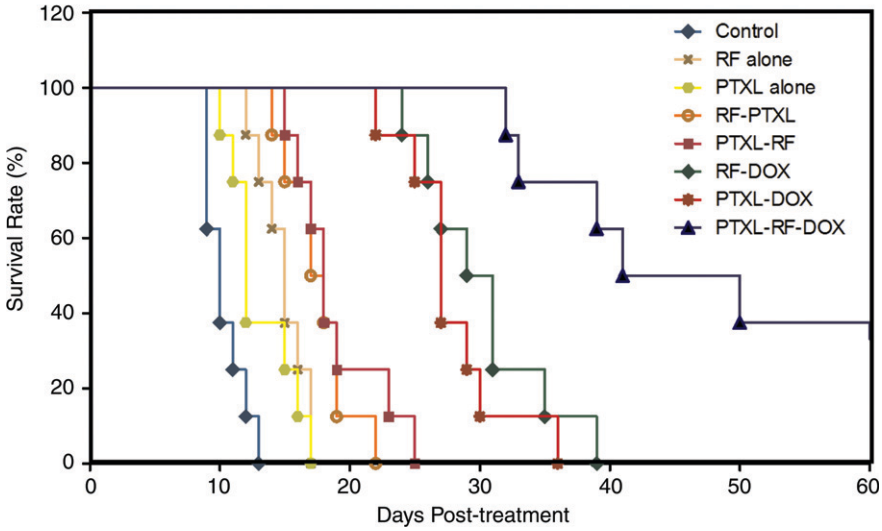

Figure 4: Kaplan-Meier analysis of animal end-point survival following treatment with RF ablation *(RF)* alone, paclitaxel *(PTXL)* alone, RF ablation–paclitaxel *(RF-PTXL)* or paclitaxel–RF ablation *(PTXL-RF)*, RF ablation–doxorubicin *(RF-DOX)*, paclitaxel and doxorubicin combined *(PTXL-DOX),* and paclitaxel–RF ablation–doxorubicin *(PTXL-RF-DOX)*. Animal end-point survival was defined as tumor diameter greater than 3.0 cm, or survival to 90 days, whichever came first. Graph was truncated at 60 days, as the final two animals had complete local control or tumor regression and survived beyond 90 days. Mean survival for animals that received RF ablation and single-agent therapy (paclitaxel–RF ablation, RF ablation–paclitaxel, or RF ablation–doxorubicin) was greater than that for animals that received RF ablation alone (14.9 days ± 1.8), for animals that received paclitaxel alone (13.1 days ± 2.5), or for control group animals (10.4 days ± 1.5; $P < .02$, all comparisons). Greatest mean end-point survival was observed with paclitaxel–RF ablation–doxorubicin (56.8 days ± 25.3; $P < .002$, all comparisons).

hyperthermia has been used to increase the effectiveness of chemotherapy by increasing blood flow, membrane permeability, local drug uptake, and metabolism in solid tumors (38,39). For example, we and others (16,18) have described the coadministration of intravenous liposomal doxorubicin with RF ablation in multiple tumor types, animal models, and a pilot clinical series. Benefits of this combination therapy over either RF ablation or liposomal doxorubicin alone include increased coagulation necrosis, increased intratumoral drug delivery predominantly in the peripheral periablation zone where sublethal tissue heating occurs, and increased animal end-point survival (15,27). Most recently, Solazzo et al (28) investigated the potential mechanisms underlying this observed synergy between RF ablation and IV liposomal doxorubicin, and by using IHC staining, they identified various levels of increased apoptosis, oxidative and nitrative cellular stress, and HSP production. As a next step, in our study, we investigated the potential role of liposomal paclitaxel, with known proapoptotic and anti-HSP effects, in RF ablation–induced tumor coagulation, intratumoral drug accumulation, and tumor growth. Our study represents an attempt to investigate the potential role of a specific modifier of cellular stress pathways, such as paclitaxel, as an adjuvant for tumor ablation and to achieve a more mechanistic-based, selective effectiveness.

Our study demonstrates that adjuvant liposomal paclitaxel increases RF ablation–induced tumor coagulation over RF ablation alone, with gains similar to those observed when RF ablation and liposomal doxorubicin are combined (18). In addition, our findings also confirm that the timing of drug and RF ablation administration can affect coagulation and that timing varies in an agent-specific manner. For example, paclitaxel administered 24 hours before RF ablation resulted in a larger amount of coagulation at 24 hours after treatment compared with administration of paclitaxel immediately after performing RF ablation. Nevertheless, ultimately, both methods of administration resulted in a similar amount of coagulation at 96 hours, such that the later administration of paclitaxel (15 minutes after RF ablation) increased tumor destruction in a delayed fashion (ie, in the 24–72-hour range). This may have occurred either through increased apoptosis or mitotic spindle inhibition. Regardless, this result suggests that paclitaxel likely requires 24 hours to increase cellular susceptibility to heat-related injury, regardless of the regimen. Such differences in optimal drug administration time likely reflect the different drug mechanisms and time required to increase cellular susceptibility (ie, priming the tumor cells for combination therapy).

We also observed markedly greater (more than 10-fold) intratumoral paclitaxel when RF ablation was added to liposomal paclitaxel alone. This corresponds to prior work demonstrating increased intratumoral liposomal doxorubicin accumulation when it is combined with RF ablation. For example, Goldberg et al (18) and Monsky et al (30) documented up to a 5.6-fold increase in intratumoral doxorubicin accumulation following RF ablation in rat breast adenocarcinoma tumor. Several mechanisms have been proposed to explain this observed effect, including hyperthermia-induced increased vascular permeability likely as a result of endothelial injury and increased reperfusion after reversible vascular stasis in the zone of tissue immediately surrounding the central ablation (a peripheral zone that has been shown to undergo exposure to sublethal temperatures) (27,38,40). Interestingly, our results also highlight the balance needed between the timing of delivery of the agent (ie, providing sufficient time to sensitize tumor cells prior to RF ablation) versus achieving maximal intratumoral concentrations. Indeed, waiting 15 minutes after RF ablation to administer paclitaxel resulted in the greatest intratumoral drug accumulation, reflecting matched peak drug

Figure 5

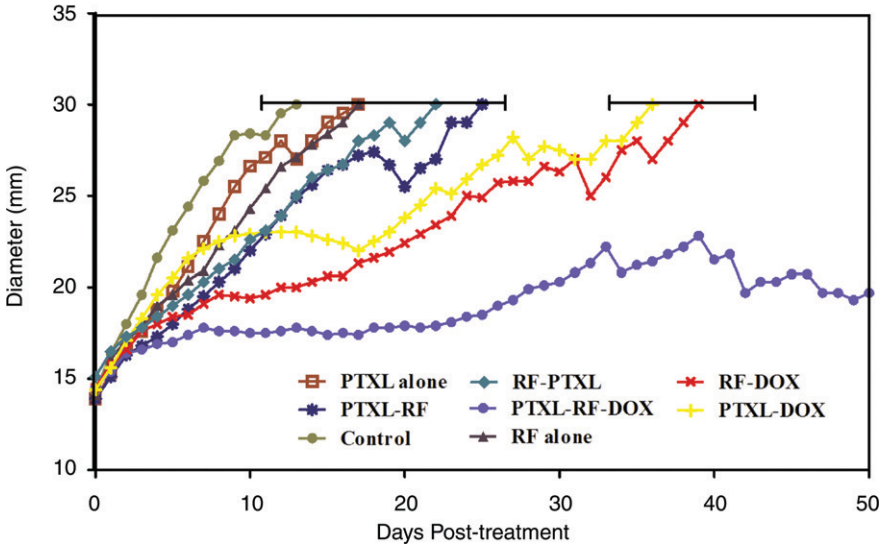

Figure 5: Tumor growth following treatment with RF ablation and/or intravenous adjuvant liposomal chemotherapy (doxorubicin or paclitaxel). Scatterplot shows mean (and final standard deviation) tumor diameter to sacrifice at 3.0-cm diameter. Combination RF ablation and a single adjuvant therapy (paclitaxel–RF ablation, RF ablation–paclitaxel, RF ablation–doxorubicin) resulted in slower tumor growth and longer survival compared with untreated or RF ablation alone groups ($P < .02$). RF ablation–doxorubicin and paclitaxel-doxorubicin groups had greater survival compared with paclitaxel–RF ablation or RF ablation–paclitaxel groups. Paclitaxel–RF ablation–doxorubicin showed the greatest survival benefit, with mean end-point survival of 56.8 days ± 25.3 ($P < .002$, all comparisons). Graph was truncated at 50 days after treatment (similar survival is observed for the surviving animals from 60 to 90 days). Keys are the same as for Figure 4.

circulation levels and hyperthermic tissue effects (ie, greatest endothelial leakiness). Nevertheless, despite the fact that paclitaxel administered 24 hours before RF ablation (paclitaxel–RF ablation) resulted in increased but comparatively lesser amounts of intratumoral drug, more rapid coagulation was observed. Regardless, similar amounts of overall coagulation and animal end-point survival were observed for both groups. This suggests that there may be a threshold effect for both drug concentration and geographic intratumoral drug distribution, beyond which only limited gains in coagulation or end-point survival are seen despite larger amounts of drug delivery.

In our study, we investigated and compared the effect of both liposomal paclitaxel and doxorubicin on RF ablation–induced apoptosis and HSP production. Our results identified different peak times and intensities for apoptosis production for doxorubicin (predominantly early after RF ablation) compared with paclitaxel (greatest effect at 24 hours after RF ablation). One possible explanation of this observed temporal variability is the difference in the mechanism of action between doxorubicin and paclitaxel. Specifically, doxorubicin prevents resealing of the DNA double helix and, therefore, replication during the interphase portion of the cell cycle (41). Paclitaxel, on the other hand, interferes with the normal function of microtubule breakdown during the mitosis phase (42). Differences in the time required to see peak antiapoptotic effects may represent differences in hyperthermic repair mechanisms (ie, DNA repair occurs earlier and microtubule repair, later).

On the basis of prior work identifying increased HSP production peripheral to the coagulation zone, we also investigated the potential role of modulating HSP production. Solazzo et al (28) previously demonstrated increased staining for HSP production (HSP70, specifically) peripheral to the treatment zone. Induction of HSP production has been associated with increased cellular resistance and thermotolerance, and paclitaxel has been shown to inhibit expression of certain HSP production over other antineoplastic agents. In this study, paclitaxel suppressed HSP70 production early (approximately 4 hours) compared with increases seen with doxorubicin here and in other studies, with less HSP suppression at later time points (approximately 24 hours). There are several possible explanations for this finding. First, the HSP suppressive effect of paclitaxel may be temporally limited. Early HSP suppression by paclitaxel may not have been able to keep up with progressive increases in HSP production, suggesting a role for either longer-acting HSP suppression or a multiple-dosing algorithm to maximize paclitaxel's proapoptotic and HSP-suppressive effects. In addition, liposome deposition occurs predominantly within the periablational tumor, such that HSP suppression may be limited by lack of significant deposition farther away from the RF ablation zone. Nevertheless, the presence of residual HSP production at all times suggests that further investigation into additional methods of HSP suppression is still warranted.

Significant differences in animal end-point survival were identified for RF ablation combined with paclitaxel over RF ablation alone. Surprisingly, longer survival was more commonly seen with regimens that included liposomal doxorubicin compared with liposomal paclitaxel (with or without RF ablation), despite differences in apoptosis, HSP70 production, and coagulation that would have seemed to favor paclitaxel. This significant survival benefit for liposomal doxorubicin over liposomal paclitaxel is likely multifactorial. Both agents have different mechanisms of action, and doxorubicin is likely more effective in this particular tumor type (a breast adenocarcinoma, for which doxorubicin is a first-line therapy in humans). Increased coagulation and animal end-point survival for RF ablation combined with liposomal doxorubicin treatments compared with RF ablation combined with paclitaxel despite its

increased apoptosis, suggests that alternate mechanisms in addition to apoptosis are important in achieving slower tumor growth rates and/or complete tumor death following ablation. Interestingly, the greatest survival occurred with paclitaxel–RF ablation–doxorubicin compared with all other therapies. Paclitaxel-induced HSP suppression may be at least partially responsible for the synergy observed between doxorubicin and paclitaxel. Regardless, the use of two agents that target separate portions of the cell cycle may be an effective strategy owing to both the potential synergy and limited cross-resistance between them.

As noted, one finding in our study was the discordance in results between tumor coagulation, intratumoral drug accumulation, and end-point animal survival, underscoring the need to carefully address the most relevant end points. This again underscores that end-point survival and delayed evaluation of tumor coagulation must be viewed as primary outcome measures. Thus, although early evaluation of coagulation diameter can help identify temporal differences between groups, the actual time it takes for a full effect to take place may vary. Hence, the determination of a full dose-response curve likely needs to be tailored for each agent and may make comparisons between different drugs even more difficult. Similarly, differences between intratumoral drug accumulation and coagulation demonstrate that identifying the drug concentration required for a threshold effect requires continued investigation.

There were several limitations in our study. Although this tumor model was selected because it is a well-characterized vascular solid adenocarcinoma (16,29), careful interpretation of the results is required. Although we purposefully selected a liposomal paclitaxel formulation that allowed us to make optimal comparisons with liposomal doxorubicin, a liposomal paclitaxel formulation similar to the one used in our study is not currently available in a Food and Drug Administration–approved form for clinical use, making rapid translation of our results into clinical practice more difficult. In addition, the differences identified between doxorubicin- and paclitaxel-based regimens likely reflect underlying tumor susceptibility to each of these agents for this particular model. Thus, further confirmation of these findings will be required in other models. Nevertheless, given the number of reports in existing literature about the use of hyperthermia in cancer therapy (43), the interaction of heat-based tissue effects and cellular reparative mechanisms will likely have a protean manifestation across multiple tumor cell lines. In addition, although we demonstrated the potential importance of drug delivery timing as it relates to RF application by using single-drug dosing regimens, further investigation into using multidose regimens and identifying the optimal balance between achieving high intratumoral drug concentrations and maximum drug effects is still required.

In conclusion, RF ablation combined with adjuvant liposomal drugs can take advantage of apoptosis and HSP inhibition to achieve more complete tumor treatment and greater survival. Our results demonstrate that combining RF ablation with adjuvant liposomal drug therapies increases intratumoral drug delivery and tumor coagulation over RF ablation or drug therapies alone. Use of a liposomal agent such as paclitaxel to target specific cellular mechanisms to increase apoptosis and suppression of HSP production can increase tumor coagulation. Our study also highlights the potential significant end-point survival benefit by combining an increasing number of adjuvant therapies (ie, two nanodrugs with RF ablation as opposed to single adjuvant agents), given that the greatest tumor coagulation and end-point survival were produced with three combined therapies. This underscores the potential synergy between administering adjuvant liposomal doxorubicin and paclitaxel together in combination with RF ablation.

Practical applications: Combining RF ablation with single or multiple adjuvant liposomal chemotherapies has the potential for further improving the role of combination therapies in interventional oncology. Our results suggest specific cellular mechanisms such as apoptosis and HSP production can be targeted to increase overall tumor destruction. In addition, we believe there is potential in clinical practice for combining RF ablation with multiple adjuvant agents that have different mechanisms of action to improve tumor treatment over the use of a single agent alone.

References

1. Dodd GD 3rd, Soulen MC, Kane RA, et al. Minimally invasive treatment of malignant hepatic tumors: at the threshold of a major breakthrough. RadioGraphics 2000;20(1):9–27.
2. Gervais DA, McGovern FJ, Arellano RS, McDougal WS, Mueller PR. Radiofrequency ablation of renal cell carcinoma. I. Indications, results, and role in patient management over a 6-year period and ablation of 100 tumors. AJR Am J Roentgenol 2005;185(1):64–71.
3. Goldberg SN, Dupuy DE. Image-guided radiofrequency tumor ablation: challenges and opportunities. I. J Vasc Interv Radiol 2001;12(9):1021–1032.
4. Lencioni R, Crocetti L, Cioni R, et al. Response to radiofrequency ablation of pulmonary tumours: a prospective, intention-to-treat, multicentre clinical trial (the RAPTURE study). Lancet Oncol 2008;9(7):621–628.
5. Lencioni R, Cioni D, Crocetti L, et al. Early-stage hepatocellular carcinoma in patients with cirrhosis: long-term results of percutaneous image-guided radiofrequency ablation. Radiology 2005;234(3):961–967.
6. Livraghi T, Goldberg SN, Lazzaroni S, et al. Hepatocellular carcinoma: radio-frequency ablation of medium and large lesions. Radiology 2000;214(3):761–768.
7. Solbiati L, Livraghi T, Goldberg SN, et al. Percutaneous radio-frequency ablation of hepatic metastases from colorectal cancer: long-term results in 117 patients. Radiology 2001;221(1):159–166.
8. Yang W, Chen MH, Wang MQ, et al. Combination therapy of radiofrequency ablation and transarterial chemoembolization in recurrent hepatocellular carcinoma after hepatectomy compared with single treatment. Hepatol Res 2009;39(3):231–240.
9. Yang W, Chen MH, Yin SS, et al. Radiofrequency ablation of recurrent hepatocellular carcinoma after hepatectomy: therapeutic efficacy on early- and late-phase recurrence. AJR Am J Roentgenol 2006;186(5 suppl):S275–S283.

10. Chopra S, Dodd GD 3rd, Chintapalli KN, Leyendecker JR, Karahan OI, Rhim H. Tumor recurrence after radiofrequency thermal ablation of hepatic tumors: spectrum of findings on dual-phase contrast-enhanced CT. AJR Am J Roentgenol 2001;177(2):381–387.

11. Siperstein A, Garland A, Engle K, et al. Local recurrence after laparoscopic radiofrequency thermal ablation of hepatic tumors. Ann Surg Oncol 2000;7(2):106–113.

12. Horkan C, Dalal K, Coderre JA, et al. Reduced tumor growth with combined radiofrequency ablation and radiation therapy in a rat breast tumor model. Radiology 2005; 235(1):81–88.

13. Lencioni R, Crocetti L, Petruzzi P, et al. Doxorubicin-eluting bead-enhanced radiofrequency ablation of hepatocellular carcinoma: a pilot clinical study. J Hepatol 2008; 49(2):217–222.

14. Grieco CA, Simon CJ, Mayo-Smith WW, DiPetrillo TA, Ready NE, Dupuy DE. Percutaneous image-guided thermal ablation and radiation therapy: outcomes of combined treatment for 41 patients with inoperable stage I/II non-small-cell lung cancer. J Vasc Interv Radiol 2006;17(7):1117–1124.

15. D'Ippolito G, Ahmed M, Girnun GD, et al. Percutaneous tumor ablation: reduced tumor growth with combined radio-frequency ablation and liposomal doxorubicin in a rat breast tumor model. Radiology 2003;228(1): 112–118.

16. Ahmed M, Liu Z, Lukyanov AN, et al. Combination radiofrequency ablation with intratumoral liposomal doxorubicin: effect on drug accumulation and coagulation in multiple tissues and tumor types in animals. Radiology 2005;235(2):469–477.

17. Ahmed M, Lukyanov AN, Torchilin V, Tournier H, Schneider AN, Goldberg SN. Combined radiofrequency ablation and adjuvant liposomal chemotherapy: effect of chemotherapeutic agent, nanoparticle size, and circulation time. J Vasc Interv Radiol 2005;16(10):1365–1371.

18. Goldberg SN, Kamel IR, Kruskal JB, et al. Radiofrequency ablation of hepatic tumors: increased tumor destruction with adjuvant liposomal doxorubicin therapy. AJR Am J Roentgenol 2002;179(1):93–101.

19. Demidenko ZN, Vivo C, Halicka HD, et al. Pharmacological induction of Hsp70 protects apoptosis-prone cells from doxorubicin: comparison with caspase-inhibitor- and cycle-arrest-mediated cytoprotection. Cell Death Differ 2006;13(9):1434–1441.

20. Du XL, Jiang T, Wen ZQ, Gao R, Cui M, Wang F. Silencing of heat shock protein 70 expression enhances radiotherapy efficacy and inhibits cell invasion in endometrial cancer cell line. Croat Med J 2009;50(2):143–150.

21. Chen H, Yu YY, Zhang MJ, et al. Protective effect of doxorubicin induced heat shock protein 72 on cold preservation injury of rat livers. World J Gastroenterol 2004;10(9): 1375–1378.

22. Frasci G, Comella P, Rinaldo M, et al. Preoperative weekly cisplatin-epirubicin-paclitaxel with G-CSF support in triple-negative large operable breast cancer. Ann Oncol 2009; 20(7):1185–1192.

23. Tanaka Y, Fujiwara K, Tanaka H, Maehata K, Kohno I. Paclitaxel inhibits expression of heat shock protein 27 in ovarian and uterine cancer cells. Int J Gynecol Cancer 2004; 14(4):616–620.

24. Yu DH, Lu Q, Xie J, Fang C, Chen HZ. Peptide-conjugated biodegradable nanoparticles as a carrier to target paclitaxel to tumor neovasculature. Biomaterials 2010;31(8): 2278–2292.

25. Crosasso P, Ceruti M, Brusa P, Arpicco S, Dosio F, Cattel L. Preparation, characterization and properties of sterically stabilized paclitaxel-containing liposomes. J Control Release 2000;63(1-2):19–30.

26. Koudelka S, Turánek-Knötigová P, Masek J, et al. Liposomes with high encapsulation capacity for paclitaxel: preparation, characterisation and in vivo anticancer effect. J Pharm Sci 2010;99(5):2309–2319.

27. Ahmed M, Monsky WE, Girnun G, et al. Radiofrequency thermal ablation sharply increases intratumoral liposomal doxorubicin accumulation and tumor coagulation. Cancer Res 2003;63(19):6327–6333.

28. Solazzo SA, Ahmed M, Schor-Bardach R, et al. Liposomal doxorubicin increases radiofrequency ablation–induced tumor destruction by increasing cellular oxidative and nitrative stress and accelerating apoptotic pathways. Radiology 2010;255(1):62–74.

29. Goldberg SN, Kruskal JB, Oliver BS, Clouse ME, Gazelle GS. Percutaneous tumor ablation: increased coagulation by combining radio-frequency ablation and ethanol instillation in a rat breast tumor model. Radiology 2000;217(3):827–831.

30. Monsky WL, Kruskal JB, Lukyanov AN, et al. Radio-frequency ablation increases intratumoral liposomal doxorubicin accumulation in a rat breast tumor model. Radiology 2002;224(3):823–829.

31. Goldberg SN, Saldinger PF, Gazelle GS, et al. Percutaneous tumor ablation: increased necrosis with combined radio-frequency ablation and intratumoral doxorubicin injection in a rat breast tumor model. Radiology 2001;220(2):420–427.

32. D'Souza GG, Wang T, Rockwell K, Torchilin VP. Surface modification of pharmaceutical nanocarriers with ascorbate residues improves their tumor-cell association and killing and the cytotoxic action of encapsulated paclitaxel in vitro. Pharm Res 2008;25(11): 2567–2572.

33. Kim SC, Yu J, Lee JW, Park ES, Chi SC. Sensitive HPLC method for quantitation of paclitaxel (Genexol®) in biological samples with application to preclinical pharmacokinetics and biodistribution. J Pharm Biomed Anal 2005;39(1-2):170–176.

34. Liszczak TM, Hedley-Whyte ET, Adams JF, et al. Limitations of tetrazolium salts in delineating infarcted brain. Acta Neuropathol (Berl) 1984;65(2):150–157.

35. Goldberg SN, Gazelle GS, Compton CC, Mueller PR, Tanabe KK. Treatment of intrahepatic malignancy with radiofrequency ablation: radiologic-pathologic correlation. Cancer 2000;88(11):2452–2463.

36. Liu X, Zou H, Slaughter C, Wang X. DFF, a heterodimeric protein that functions downstream of caspase-3 to trigger DNA fragmentation during apoptosis. Cell 1997; 89(2):175–184.

37. Thériault JR, Adachi H, Calderwood SK. Role of scavenger receptors in the binding and internalization of heat shock protein 70. J Immunol 2006;177(12):8604–8611.

38. Kong G, Braun RD, Dewhirst MW. Characterization of the effect of hyperthermia on nanoparticle extravasation from tumor vasculature. Cancer Res 2001;61(7):3027–3032.

39. Gnant MF, Noll LA, Terrill RE, et al. Isolated hepatic perfusion for lapine liver metastases: impact of hyperthermia on permeability of tumor neovasculature. Surgery 1999;126(5):890–899.

40. Yuan F, Dellian M, Fukumura D, et al. Vascular permeability in a human tumor xenograft: molecular size dependence and cutoff size. Cancer Res 1995;55(17):3752–3756.

41. Fornari FA, Randolph JK, Yalowich JC, Ritke MK, Gewirtz DA. Interference by doxorubicin with DNA unwinding in MCF-7 breast tumor cells. Mol Pharmacol 1994; 45(4):649–656.

42. Horwitz SB. Mechanism of action of taxol. Trends Pharmacol Sci 1992;13(4):134–136.

43. Moyer HR, Delman KA. The role of hyperthermia in optimizing tumor response to regional therapy. Int J Hyperthermia 2008; 24(3):251–261.